Title: Rifapentine population pharmacokinetics and dosing recommendations for latent tuberculosis infection

Authors: Jennifer E. Hibma, Pharm.D.*[1], Kendra K. Radtke, Pharm.D.*[1], Susan E. Dorman, M.D.[4], Amina Jindani, M.D. F.R.C.P[3], Kelly E. Dooley, M.D. Ph.D.[4], Marc Weiner, M.D.[5], Helen M. McIlleron, Ph.D.[2], Radojka M. Savic, Ph.D.[1#]

* Contributed equally.

Affiliations: [1] Department of Bioengineering & Therapeutic Sciences, University of California, San Francisco, California, United States; [2] Division of Clinical Pharmacology, Department of Medicine, University of Cape Town, South Africa; [3] St. George's, University of London, United Kingdom; [4] Johns Hopkins University School of Medicine, Baltimore, Maryland, United States; [5] University of Texas Health Science Center at San Antonio and the South Texas VAMC, San Antonio, Texas

[#]**Corresponding Author:** Rada M. Savic [1700 4th St, Rm 503C, UCSF Box 2552 San Francisco, CA 94158, United States, +1 415 502 0640, and rada.savic@ucsf.edu]

Short running title: Pooled analysis of rifapentine pharmacokinetics

Impact Statement: Our model is the first to characterize rifapentine population pharmacokinetics with concentration-driven autoinduction and includes all clinically relevant patient factors. We show evidence to support removing weight band dosing from rifapentine dosing guidelines and propose increased doses for individuals with HIV. This model will serve as an important tool for determining optimal rifapentine doses for tuberculosis infection and active disease in future clinical trials and clinical practice.

Descriptor number: 11.06 Treatment of Tuberculosis or Latent Infection

Manuscript word count: 2355/3500

"This article has an online data supplement, which is accessible from this issue's table of content online at **www.atsjournals.org**"

"At a Glance Commentary"

What is the current scientific knowledge on this subject?

Rifapentine has become a principle component of novel short-course regimens for latent tuberculosis infection and a promising agent for treatment shortening regimens for active disease. Evidence suggests that rifapentine induces its own elimination, but the implications for novel dosing strategies are not well understood. Further, the evidence supporting the current weight band dosing of rifapentine is lacking and requires further evaluation.

What does this study add to the field?

In this individual participant data meta-analysis of rifapentine pharmacokinetics, we describe the population pharmacokinetics of rifapentine, including full characterization of the autoinduction profile. We find no evidence supporting weight band dosing of rifapentine and thus, recommend all individuals receive the same dose, with the exception of HIV-positive individuals, who would benefit from higher doses. This model will serve as a valuable tool for predicting drug exposure and determining optimal rifapentine doses for future clinical trials and in clinical practice.

1   **Abstract**

2

3   **Rationale:** Rifapentine has been investigated at various doses, frequencies, and dosing

4   algorithms but clarity on the optimal dosing approach is lacking.

5   **Objectives:** In this individual participant data meta-analysis of rifapentine pharmacokinetics, we

6   characterize rifapentine population pharmacokinetics, including autoinduction, and determine

7   optimal dosing strategies for short-course rifapentine-based regimens for latent tuberculosis

8   infection.

9   **Methods:** Rifapentine pharmacokinetic studies were identified though a systematic review of

10   literature. Individual plasma concentrations were pooled, and non-linear mixed effects modeling

11   was performed. A subset of data was reserved for external validation. Simulations were

12   performed under various dosing conditions including current weight-based methods and

13   alternative methods driven by identified covariates.

14   **Measurements and Main Results:** We identified 9 clinical studies with a total of 863

15   participants with pharmacokinetic data (n=4301 plasma samples). Rifapentine population

16   pharmacokinetics were described successfully with a one-compartment distribution model.

17   Autoinduction of clearance was driven by rifapentine plasma concentration. The maximum effect

18   was a 72% increase in clearance and was reached after 21 days. Drug bioavailability decreased

19   by 27% with HIV infection, decreased by 28% with fasting, and increased by 49% with a high-

20   fat meal. Body weight was not a clinically relevant predictor of clearance. Pharmacokinetic

21   simulations showed that current weight-based dosing leads to lower exposures in low weight

22   individuals, which can be overcome with flat dosing. In HIV-positive patients, 30% higher doses

23   are required to match drug exposure in HIV-negative patients.

24   **Conclusions:** Weight-based dosing of rifapentine should be removed from clinical guidelines

25   and higher doses for HIV-positive patients should be considered to provide equivalent efficacy.

26

27   **Abstract word count:** 250/250

28

29   **Keywords:** tuberculosis; rifapentine; rifamycins; population pharmacokinetics; latent

30   tuberculosis

Introduction

The World Health Organization (WHO) estimates that 23% of the world's population has latent tuberculosis infection (LTBI) and is at risk of developing active disease (1). Standard treatment for LTBI has historically been 9 months of daily isoniazid, for which patient compliance is poor and hepatotoxicity is a concern (2, 3). Recently, novel rifapentine-based regimens have demonstrated efficacy in preventing tuberculosis disease with much shorter treatment durations. (4, 5). Additionally, these regimens have shown equal to better safety profiles and higher patient compliance. The first regimen was three months of once-weekly rifapentine plus isoniazid (3HP) (4); it received FDA approval in 2014 and is now recommended by the Centers for Disease Control and the WHO for individuals with LTBI (6-8). An ultra-short-course regimen, one month of daily isoniazid-rifapentine (1HP), has also shown efficacy, safety, and improved compliance in HIV-infected patients at high risk of developing tuberculosis disease (5); 1HP inclusion into WHO guidelines is under review (9).

Rifapentine has high anti-mycobacterial activity and a long elimination half-life of 15 hours that makes it an attractive candidate for treatment shortening regimens (6, 10, 11). However, unlike in LTBI, it is still unknown if rifapentine will be effective in short-course regimens for active drug-sensitive tuberculosis disease (DS-TB). The only completed Phase 3 clinical trial (Rifaquin) failed to demonstrate non-inferiority of intermittent rifapentine regimens in DS-TB patients compared to the 6-month standard of care (12).

Robust characterization of rifapentine pharmacokinetics is required to determine optimal dosing strategies for new short-course regimens and for special populations. Current rifapentine-based

54 regimens for LTBI use weight band dosing (6, 8). However, these recommendations are not

55 based on pharmacokinetic evidence; rather, they are drawn from the historical mg/kg doses used

56 in rifampin-based therapy. The influence of body weight on rifapentine clearance remains

57 inconclusive as current studies report conflicting findings (13, 14). Meal-type, dose amount, HIV

58 status, race, and age may also impact rifapentine concentration (14-18). Additionally, repeated

59 dosing of twice weekly and daily administration results in lower rifapentine exposures over time,

60 suggesting that rifapentine induces its own metabolism (19, 20).

61

62 Several Pharmacokinetic studies have been conducted with varying rifapentine doses (up to 20

63 mg/kg daily), frequencies (once weekly to twice daily), and methods (weight-based or flat dose)

64 (19-22). Our aim here was to perform an individual participant data meta-analysis and pool

65 individual pharmacokinetic data from all relevant clinical studies in various populations (healthy

66 volunteers and LTBI and DS-TB patients with and without HIV infection). The goals are (i) to

67 characterize rifapentine population pharmacokinetics, including the time course of autoinduction

68 and relevant covariates that may have a significant clinical impact on rifapentine exposures and

69 clinical efficacy, and (ii) to derive dosing recommendations to inform optimal current and future

70 use of rifapentine in tuberculosis infection and disease.

71

72 **Methods**

73 **Clinical Studies**

74 Rifapentine pharmacokinetic studies were identified through a literature search in PubMed with

75 the terms 'rifapentine' AND ('study' OR 'trial') from 1 January 1980 to 31 December 2015

76 according to PRISMA guidelines (23). Additional studies were identified through author

4

77 collaborations. Corresponding authors of the study were invited to contribute data if the studies

78 were prospective and multiple dose, pharmacokinetic measurements were available and

79 validated, and covariates of interest were documented (e.g., HIV status, meal-type, and weight).

80 All studies included in the analysis received ethical approval by their local ethical review boards.

81

82 **Population Pharmacokinetic Analysis**

83 Identified studies were split into an analysis cohort for structural model development and a

84 validation cohort for external validation. We sought to conserve 1/3 of drug concentration data

85 for the validation cohort and to match dosing schedules and covariates (eg, HIV) between

86 cohorts when possible. Rifapentine plasma concentrations were natural log-transformed and

87 analyzed using non-linear mixed effects modeling with NONMEM 7.41 (ICON Development

88 Solutions, Elliott City, Maryland). Pharmacokinetic data without an associated dosing record

89 were excluded.

90

91 Population pharmacokinetic model building followed standard procedures by first characterizing

92 the base structural model (24). To describe rifapentine autoinduction, a semi-mechanistic

93 enzyme turnover model was used (25). Known covariate effects (i.e., HIV, meal-type, dose)

94 were incorporated into the structural model. Additional covariate effects such as weight, age,

95 race, BMI and sex were identified through a stepwise procedure with forward selection ($p<0.05$)

96 and backward elimination ($p<0.01$). Final inclusion of covariates was based on statistical

97 significance, scientific plausibility, and clinical relevance defined as $\geq 20\%$ change in the

98 parameter estimate (26). Model development was guided by graphical assessment of goodness-

99 of-fit plots, condition number, and the likelihood ratio test. Simulation-based diagnostics (e.g.,

100   visual predictive check [VPC]) were used for model validation. Detailed model building

101   procedures are provided in the Supplemental material.

102

103   **Software**

104   R software (version 3.4.2) was used for all data management, analyses, and graphical

105   visualization. The xpose (version 0.4.4) and vpc (version 1.0.1) packages were used for visual

106   diagnostics. Nonparametric bootstrap and covariate modeling were performed with Perl-speaks-

107   NONMEM (version 4.7.0).

108

109   **Dosing simulations**

110   Simulations were performed with the final model to (i) predict the autoinduction process with

111   different doses and dosing schedules, (ii) assess the impact of clinically relevant patient factors

112   (e.g., HIV, weight) on rifapentine exposure, and (iii) to propose pragmatic dosing for rifapentine-

113   containing LTBI regimens. Pharmacokinetic profiles were evaluated by different drivers of

114   pharmacodynamics, including time above minimum inhibitory concentration (MIC), area under

115   the concentration-time curve (AUC), AUC/MIC, maximum concentration (C_{max}), and C_{max}/MIC,

116   with MIC set to 0.06 mg/L (27). For 1HP and 3HP simulations, we predicted rifapentine

117   exposure following current weight band dosing (1HP: 300 mg [<35 kg], 450 mg [35-45 kg], or

118   600 mg [>45 kg] daily; 3HP: 750 mg [<50 kg] and 900 mg [≥50 kg] once weekly) (4, 5).

119   Alternative dosing methods were explored based on identified covariates. All simulations were

120   performed under low-fat meal conditions (the referent, where relative bioavailability =1) given

121   label recommendations.

122

123 **Univariate analysis of month 2 culture conversion**

124 Microbiological outcome data (i.e., liquid and solid culture data) was acquired from two Phase II

125 clinical studies: TBTC-29 and TBTC-29x (22, 28). Participant body weight and rifapentine AUC

126 were evaluated as predictors month 2 culture conversion by logistic regression. Body weight was

127 categorized as < 50 kg or ≥ 50 kg, consistent with the weight band dosing strategy used in these

128 studies. AUC was categorized at the median AUC.

129

130

131 **Results**

132 **Clinical Studies**

133 We identified nine clinical studies with rifapentine pharmacokinetic data for the pooled analysis

134 (Figure 1), including Phase 3 (n=2), Phase 2 (n=4), and Phase 1 (n=3) studies (12, 14, 19-21, 28-

135 31). Overall, 863 subjects were included: 84 healthy volunteers, 702 patients with DS-TB, and

136 77 persons treated for LTBI. The analysis cohort included 360 subjects (n=3273 samples) from

137 five studies. The validation cohort included 503 subjects (n=1115 samples) from four studies.

138 Participant and trial characteristics are shown in Table 1. The analysis and validation cohorts

139 were similar in design and participant characteristics. Overall, the median age was 34 years, the

140 median weight was 59 kg, 31% were men, and 9% of patients were HIV-positive. There was a

141 wide range of rifapentine doses, dosing frequencies, and diets that were tested across studies

142 (Table 1).

143

144 **Pharmacokinetic-enzyme model**

145   The final rifapentine pharmacokinetic-enzyme model is shown in Figure 2, and final parameter

146   estimates are in Table 2. All pharmacokinetic parameters were well estimated with low relative

147   standard errors. Rifapentine apparent clearance was estimated to be 1.11 L/h in the typical adult

148   and increased up to 1.92 L/h (173%) over time as a result of autoinduction. The induction

149   process was described using an indirect response semi-mechanistic enzyme turnover model

150   (Figure 2). The effect (EFF) of rifapentine drug concentration on enzyme production was

151   described through an E_{max} relationship:

152
$$EFF = \left(\frac{E_{max} \cdot C_p{}^{\gamma}}{EC_{50}{}^{\gamma} + C_p{}^{\gamma}} \right)$$

153   where EC_{50} is the rifapentine concentration in plasma (C_p) when half the maximum induction

154   effect (E_{max}) is observed; γ represents the steepness of the relationship. The maximum

155   autoinduction effect is expected at the steady state concentrations achieved with daily doses of

156   300 mg or more, and clearance stabilizes by day 21 of therapy, assuming 5 half-lives to steady

157   state (Figure 3).

158
159   **Rifapentine model evaluation and validation**

160   The VPC of the basic structural model (built with analysis cohort data alone) shows that the

161   model predicted the analysis cohort raw data well: the median, 5th, and 95th percentiles of raw

162   data fell within or near the percentiles of model-predicted concentrations for all time points

163   (Figure 4A). Further, we show that model-predicted concentrations matched the raw data of an

164   external dataset (i.e., the validation cohort, which was not used in model development; Figure

165   4B).

166

167   After model validation, data from both cohorts were pooled and parameters re-estimated. VPCs

168   of the final pharmacokinetic model for rifapentine and its metabolite are provided in the

169   Supplement. The final model predicted rifapentine (Figure E2) and metabolite (Figure E3)

170   concentrations well for all studies.

171

172   **Impact of covariates on rifapentine pharmacokinetics**

173   Rifapentine bioavailability was strongly (p<0.001) influenced by HIV status, food, and dose with

174   clinically relevant effect sizes. The relative effects on bioavailability of HIV-positive status (vs.

175   HIV-negative), high-fat meal or fasting condition (vs. low-fat meal), and dose per 100 mg above

176   300 mg (the referent) are shown in Table 2. Body weight was related to rifapentine clearance

177   (p<0.001) with a 0.1 L/h (9%) increase in clearance per 10 kg increase in weight (Figure 5).

178   However, weight explained only 2.9% of the inter-individual variability in clearance, and the

179   effect size did not meet our criteria for clinical relevance. Further, the majority of statistical

180   significance was from a few influential individuals over 90 kg in weight (Supplemental).

181   Allometrically scaling clearance did not provide any additional improvement over the linear

182   relationship, and the functions were nearly identical at relevant weight ranges (40-100 kg).

183   Therefore, the only covariates included in the final model were HIV, food, and dose.

184

185   **Rifapentine simulations of different dosing schedules**

186   The effect of dose and dosing frequency on rifapentine pharmacokinetics is shown in Figure 6.

187   With intermittent dosing, autoinduction was minimal to moderate and clearance increased

188   slightly with larger doses (see Supplemental). With daily dosing, maximum induction was

189   achieved with doses of 300 mg or more. All dosing schedules were able to maintain

190 concentrations above MIC during the dosing interval except once weekly in which

191 concentrations fall below MIC just prior to the next dose (Figure 6B). C_{max}/MIC and AUC/MIC

192 were highest with daily dosing, due to drug accumulation, and increased with increasing dose

193 (Online data supplement, E2 Table).

194

195 **Rifapentine simulations for 1HP and 3HP therapy**

196 We simulated rifapentine drug concentrations under the 1HP and 3HP regimens for LTBI in both

197 HIV-positive and HIV-negative adults. The typical HIV-positive patient had lower drug

198 concentrations than the typical HIV-negative patient when given the same dose due to decreased

199 rifapentine bioavailability (Figure 7). Lower drug concentrations are also predicted in low

200 weight individuals with the current weight band dosing (Figure 7). Removing weight bands and

201 administering the same flat dose to all individuals would result in equal exposures across

202 weights; however, it did not equalize exposures by HIV status (Figure 8). With a stratified

203 regimen, where HIV-positive individuals receive ~30% higher doses, similar exposures are

204 expected by HIV status and weight for both 1HP and 3HP (Figure 8).

205

206 **Univariate analysis of month 2 culture conversion**

207 A total of 363 individuals treated with 10 mg/kg rifapentine had Phase II microbiological data

208 available. Univariate logistic regression results for month 2 culture conversion of liquid media

209 are shown in Figure 9. Month 2 culture conversion was less likely in individuals who had lower

210 rifapentine AUC (Odds ratio = 0.49) and in those who weighed less than 50 kg (Odds ratio =

211 0.60).

212

Discussion

214 In this study, we used a pooled individual-data approach with an external validation to describe

215 rifapentine population pharmacokinetics in a large cohort of subjects. This analysis included nine

216 clinical studies with a wide range of rifapentine doses and scheduling frequencies, allowing for

217 successful characterization of rifapentine autoinduction with respect to drug concentration. It

218 represents the largest analysis of rifapentine population pharmacokinetics to date. Our results

219 establish several findings that may help guide rifapentine dosing strategies: (i) pharmacokinetic

220 data do not support dosing rifapentine by body weight; (ii) HIV-positive individuals require at

221 least 30% higher doses to achieve equal drug exposures to HIV-negative persons; (iii) rifapentine

222 autoinduction is strongly influenced by dosing frequency rather than dose amount.

223

224 Since rifapentine's approval, several studies have shown evidence of rifapentine inducing its

225 own elimination but none have characterized autoinduction with respect to rifapentine

226 concentration (14, 16, 17, 19, 20). Previously published models have described rifapentine

227 autoinduction empirically with time-varying clearance model (14, 17) or reduced bioavailability

228 (16). While these approaches are adequate for describing data, they have limited utility in clinical

229 settings and for dose determination in new clinical trials. In our analysis, we used a semi-

230 mechanistic turnover model where rifapentine concentration was the driver of autoinduction

231 (25). This method is advantageous in that it allows for predicting the magnitude of autoinduction

232 with different rifapentine regimens of various doses and frequencies, including those which have

233 not yet been tested in a clinical trial.

234

235   Rifapentine autoinduction is strongly influenced by dosing frequency. Simulated

236   pharmacokinetic profiles showed increasing C_{max} and AUC in the first week of therapy with

237   daily dosing due to drug accumulation but decreased thereafter as a result of clearance induction.

238   This effect was most prominent with daily dosing, moderate with thrice weekly dosing, and

239   minimal with less frequent dosing. These findings are in agreement with previous reports from

240   non-compartmental analyses (20, 30, 32). Dose amount had little effect on the magnitude of

241   autoinduction (~10% higher clearance with 1200 mg vs. 600 mg), regardless of dosing

242   frequency. A dose effect on rifapentine autoinduction has been described previously (17, 19). In

243   our model, nonproportional increases in drug exposure with increasing dose were described

244   through a reduction in bioavailability, consistent with saturable absorption (14). Still, as the

245   induction process is a function of rifapentine plasma concentration in our model, any additional

246   dose effects on clearance would be captured. While full autoinduction is predicted with daily

247   dosing, drug accumulation was also high, leading to superior C_{max}/MIC and AUC/MIC compared

248   to less frequent dosing. This confirms that daily dosing has the highest potential for

249   concentration-dependent killing of *M. tuberculosis*. Further, this work is an important

250   contribution to the understanding of the rifapentine dose-exposure relationship, especially in the

251   context of DS-TB where daily dosing is likely required (15).

252

253   Currently, body weight is the only dose determining factor for rifapentine, which was not

254   supported in our analysis. In three previously described population pharmacokinetic models,

255   weight did not influence rifapentine pharmacokinetics (15) (14, 17). Furthermore, Savic and

256   colleagues supported flat dosing of rifapentine, which was later implemented in a Phase 3

257   clinical trial for DS-TB (Study 31, Clinicaltrials.gov NCT02410772) (15). Contrarily, Langdon

258   and colleagues report a change in rifapentine clearance by 0.5 L/h per 10 kg of body weight in a

259   small cohort of 46 patients (13). However, their model did not incorporate dose-dependent

260   absorption (i.e., reduced bioavailability with increased dose), which likely would reduce the

261   estimated weight effect on clearance since the study dosed by weight, and clearance and

262   bioavailability are indirectly linked with oral dosing (13). Francis et al. allometrically scaled

263   clearance by fat-free mass (16). The model's application to rifapentine dosing, which is based on

264   total body weight, was not described. Our study is the largest population pharmacokinetic study

265   to-date with over 800 patients and healthy volunteers. While a small weight effect was observed

266   (<10% change in clearance per 10 kg in body weight), it does not justify a 150 mg (~30%)

267   change in dose as currently recommended in LTBI dosing guidelines. Weight and patient

268   population appeared correlated in our dataset (i.e., DS-TB patients weighed less on average);

269   therefore, we investigated the weight effect in healthy volunteers, individuals with LTBI, and

270   DS-TB patients separately. The weight effect was comparable and remained clinically irrelevant.

271   We conclude that weight is not a clinically relevant predictor of rifapentine clearance and that

272   weight-based dosing should not be recommended.

273

274   Simulations of the 1HP and 3HP regimens showed lower rifapentine exposures in low weight

275   individuals who receive lower doses with current weight band dosing. This ultimately puts the

276   smallest, most vulnerable individuals at risk of underexposure and consequently, treatment

277   failure (33, 34). A univariate analysis of Phase 2 culture data from two DS-TB studies showed

278   month 2 culture conversion was less likely in low weight individuals and those with low

279   rifapentine exposure. While the pharmacokinetic-pharmacodynamic relationships in LTBI have

280   not been established, rifamycins show concentration-dependent killing of *M. tuberculosis* and

281   rifapentine AUC is a strong predictor of month 2 culture conversion (15, 35). Flat dosing of

282   rifapentine (e.g., prescribing the same dose to all adults) ensures equal rifapentine exposure in

283   adult patients of all sizes and thus, equal chance of successful outcome. Moreover, flat dosing

284   simplifies the regimen in adults and encourages coformulation of rifapentine and isoniazid into a

285   fixed-dose combination tablet, reducing pill burden and simplifying the regimen even further.

286

287   Dose discrimination may be warranted by HIV status. HIV-positive persons have 27% lower

288   rifapentine bioavailability, resulting in lower exposures than HIV-negative adults. Reduced

289   bioavailability of rifamycins with HIV infection has been reported previously (15, 17) and has

290   been attributed to malabsorption (36-38). While antiretroviral drugs may also explain decreases

291   in rifamycin concentration, the HIV-positive participants in our analysis did not receive

292   antiretroviral therapy (12, 22, 28). Given rifapentine's main metabolite has activity against *M.*

293   *tuberculosis*, we also looked at metabolite concentrations by HIV status. It appeared that HIV-

294   positive individuals had lower exposures of both rifapentine and its metabolite, confirming need

295   for higher doses in HIV+ patients. Increasing the 3HP dose to 1200 mg once weekly in HIV-

296   positive patients results in similar exposures to 900 mg once weekly in HIV-negative patients.

297   Likewise, 750 mg daily in HIV-positive adults is similar to 600 mg daily in HIV-negative adults

298   for the 1HP regimen. While 1HP at 600 mg daily was effective in preventing tuberculosis disease

299   in HIV-positive individuals (5), this may reflect the minimum effective dose and higher doses

300   may provide better protection.

301

302   The proposed dosing recommendations are limited by the lack of established pharmacokinetic

303   targets in LTBI. We proposed doses that would match median exposures following the standard

304   doses tested in clinical trials with demonstrated efficacy. Given the development of tuberculosis

305   was rare in those studies, these pharmacokinetic targets are reasonable, and we would expect the

306   proposed doses to result in similar efficacy to that observed in clinical trial. The pharmacokinetic

307   target for 1HP regimen reflects the median predicted exposure in a typical HIV-positive adult

308   receiving 600 mg daily and may be on the low end. Pharmacokinetic data from BRIEF-TB and

309   future trials are urgently needed to confirm pharmacokinetic thresholds for 1HP. Additionally,

310   one study showed higher rifapentine bioavailability in Asians compared to Africans, which could

311   impact dose requirement (15). This finding could not be confirmed in our study because TBTC

312   29X was the only study contributing substantial Asian population. Further investigation of race

313   effects on rifapentine pharmacokinetics is required.

314

315   Our systematic review included all relevant studies published prior to 2016. Only one

316   pharmacokinetic study was identified in more recent literature and would not have met our

317   inclusion criteria due to non-standardized meal administration (16). Thus, our model represents

318   the most up-to-date analysis of rifapentine pharmacokinetics. Of note, the analysis includes only

319   one study in LTBI participants. To-date, these remain the only pharmacokinetic data in this

320   population. Further, there is no evidence to suggest pharmacokinetics would differ by disease

321   state, so we do not expect this to impact the generalizability of our work to LTBI treatment.

322

323   In conclusion, rifapentine exhibits autoinduction which is strongly influenced by dosing

324   frequency. Weight was not a clinically relevant predictor of rifapentine clearance; thus, dosing

325   should not be based on an individual's weight. In fact, weight-based dosing results in

326   substantially lower drug concentrations that could ultimately compromise treatment efficacy. If

327   stratified dosing is to be implemented, it should be done on the basis of HIV status to ensure that

328   HIV-positive individuals are adequately exposed to drug. Lastly, as rifapentine use becomes

329   more widespread in tuberculosis treatment and prevention, this model can serve as a useful tool

330   in clinical practice and in clinical trial design for dose determination and exposure prediction.

References

1. WHO. Global Tuberculosis Report 2018. Geneva: World Health Organization; 2018.

2. American Thoracic Society, Centers for Disease Control and Prevention. Targeted tuberculin testing and treatment of latent tuberculosis infection. *Am J Respir Crit Care Med* 2000; 161: S221-247.

3. Horsburgh CR, Jr., Goldberg S, Bethel J, Chen S, Colson PW, Hirsch-Moverman Y, Hughes S, Shrestha-Kuwahara R, Sterling TR, Wall K, Weinfurter P, Tuberculosis Epidemiologic Studies C. Latent TB infection treatment acceptance and completion in the United States and Canada. *Chest* 2010; 137: 401-409.

4. Sterling TR, Villarino ME, Borisov AS, Shang N, Gordin F, Bliven-Sizemore E, Hackman J, Hamilton CD, Menzies D, Kerrigan A, Weis SE, Weiner M, Wing D, Conde MB, Bozeman L, Horsburgh CR, Jr., Chaisson RE, Team TBTCPTS. Three months of rifapentine and isoniazid for latent tuberculosis infection. *N Engl J Med* 2011; 365: 2155-2166.

5. Swindells S, Ramchandani R, Gupta A, Benson CA, Leon-Cruz J, Mwelase N, Jean Juste MA, Lama JR, Valencia J, Omoz-Oarhe A, Supparatpinyo K, Masheto G, Mohapi L, da Silva Escada RO, Mawlana S, Banda P, Severe P, Hakim J, Kanyama C, Langat D, Moran L, Andersen J, Fletcher CV, Nuermberger E, Chaisson RE, Team BTAS. One Month of Rifapentine plus Isoniazid to Prevent HIV-Related Tuberculosis. *N Engl J Med* 2019; 380: 1001-1011.

6. FDA. Prifitin (rifapentine) Product Label. 1998 November 2014. Available from: https://www.accessdata.fda.gov/drugsatfda_docs/label/2014/021024s011lbl.pdf.

7. CDC. Treatment Regimens for Latent TB Infection (LTBI). 2016 [cited 2019 September 11]. Available from: https://www.cdc.gov/tb/topic/treatment/ltbi.htm.

8. World Health Organization. Guidelines for treatment of tuberculosis. Geneva, Switzerland: WHO Press; 2010.

9. WHO Global TB Programme. Latent tuberculosis infection: Updated and consolidated guidelines for programmatic management. Background document on the 2019 revision.; 2019.

10. Heifets LB, Lindholm-Levy PJ, Flory MA. Bactericidal activity in vitro of various rifamycins against Mycobacterium avium and Mycobacterium tuberculosis. *Am Rev Respir Dis* 1990; 141: 626-630.

11. Sirgel FA, Fourie PB, Donald PR, Padayatchi N, Rustomjee R, Levin J, Roscigno G, Norman J, McIlleron H, Mitchison DA. The early bactericidal activities of rifampin and rifapentine in pulmonary tuberculosis. *Am J Respir Crit Care Med* 2005; 172: 128-135.

12. Jindani A, Harrison TS, Nunn AJ, Phillips PP, Churchyard GJ, Charalambous S, Hatherill M, Geldenhuys H, McIlleron HM, Zvada SP, Mungofa S, Shah NA, Zizhou S, Magweta L, Shepherd J, Nyirenda S, van Dijk JH, Clouting HE, Coleman D, Bateson AL, McHugh TD, Butcher PD, Mitchison DA, Team RT. High-dose rifapentine with moxifloxacin for pulmonary tuberculosis. *N Engl J Med* 2014; 371: 1599-1608.

13. Langdon G, Wilkins J, McFadyen L, McIlleron H, Smith P, Simonsson US. Population pharmacokinetics of rifapentine and its primary desacetyl metabolite in South African tuberculosis patients. *Antimicrob Agents Chemother* 2005; 49: 4429-4436.

14. Savic RM, Lu Y, Bliven-Sizemore E, Weiner M, Nuermberger E, Burman W, Dorman SE, Dooley KE. Population pharmacokinetics of rifapentine and desacetyl rifapentine in healthy volunteers: nonlinearities in clearance and bioavailability. *Antimicrob Agents Chemother* 2014; 58: 3035-3042.

15. Savic RM, Weiner M, MacKenzie WR, Engle M, Whitworth WC, Johnson JL, Nsubuga P, Nahid P, Nguyen NV, Peloquin CA, Dooley KE, Dorman SE, Tuberculosis Trials Consortium of the Centers for Disease C, Prevention. Defining the optimal dose of rifapentine for pulmonary tuberculosis: Exposure-response relations from two phase II clinical trials. *Clin Pharmacol Ther* 2017; 102: 321-331.

16. Francis J, Zvada SP, Denti P, Hatherill M, Charalambous S, Mungofa S, Dawson R, Dorman S, Gupte N, Wiesner L, Jindani A, Harrison TS, Olagunju A, Egan D, Owen A, McIlleron HM. A Population Pharmacokinetic Analysis Shows that Arylacetamide Deacetylase (AADAC) Gene Polymorphism and HIV Infection Affect the Exposure of Rifapentine. *Antimicrob Agents Chemother* 2019; 63.

17. Zvada SP, Van Der Walt JS, Smith PJ, Fourie PB, Roscigno G, Mitchison D, Simonsson US, McIlleron HM. Effects of four different meal types on the population pharmacokinetics of single-dose rifapentine in healthy male volunteers. *Antimicrob Agents Chemother* 2010; 54: 3390-3394.

18. Keung AC, Owens RC, Jr., Eller MG, Weir SJ, Nicolau DP, Nightingale CH. Pharmacokinetics of rifapentine in subjects seropositive for the human immunodeficiency virus: a phase I study. *Antimicrob Agents Chemother* 1999; 43: 1230-1233.

19. Dooley K, Flexner C, Hackman J, Peloquin CA, Nuermberger E, Chaisson RE, Dorman SE. Repeated administration of high-dose intermittent rifapentine reduces rifapentine and moxifloxacin plasma concentrations. *Antimicrob Agents Chemother* 2008; 52: 4037-4042.

20. Dooley KE, Bliven-Sizemore EE, Weiner M, Lu Y, Nuermberger EL, Hubbard WC, Fuchs EJ, Melia MT, Burman WJ, Dorman SE. Safety and pharmacokinetics of escalating daily

doses of the antituberculosis drug rifapentine in healthy volunteers. *Clin Pharmacol Ther* 2012; 91: 881-888.

21. Dooley KE, Savic RM, Park JG, Cramer Y, Hafner R, Hogg E, Janik J, Marzinke MA, Patterson K, Benson CA, Hovind L, Dorman SE, Haas DW, Team AAS. Novel dosing strategies increase exposures of the potent antituberculosis drug rifapentine but are poorly tolerated in healthy volunteers. *Antimicrob Agents Chemother* 2015; 59: 3399-3405.

22. Dorman SE, Goldberg S, Stout JE, Muzanyi G, Johnson JL, Weiner M, Bozeman L, Heilig CM, Feng PJ, Moro R, Narita M, Nahid P, Ray S, Bates E, Haile B, Nuermberger EL, Vernon A, Schluger NW, Tuberculosis Trials C. Substitution of rifapentine for rifampin during intensive phase treatment of pulmonary tuberculosis: study 29 of the tuberculosis trials consortium. *J Infect Dis* 2012; 206: 1030-1040.

23. Moher D, Liberati A, Tetzlaff J, Altman DG, Group P. Preferred reporting items for systematic reviews and meta-analyses: the PRISMA statement. *Ann Intern Med* 2009; 151: 264-269, W264.

24. Byon W, Smith MK, Chan P, Tortorici MA, Riley S, Dai H, Dong J, Ruiz-Garcia A, Sweeney K, Cronenberger C. Establishing best practices and guidance in population modeling: an experience with an internal population pharmacokinetic analysis guidance. *CPT Pharmacometrics Syst Pharmacol* 2013; 2: e51.

25. Smythe W, Khandelwal A, Merle C, Rustomjee R, Gninafon M, Bocar Lo M, Sow OB, Olliaro PL, Lienhardt C, Horton J, Smith P, McIlleron H, Simonsson US. A semimechanistic pharmacokinetic-enzyme turnover model for rifampin autoinduction in adult tuberculosis patients. *Antimicrob Agents Chemother* 2012; 56: 2091-2098.

26. Mould DR, Upton RN. Basic concepts in population modeling, simulation, and model-based drug development-part 2: introduction to pharmacokinetic modeling methods. *CPT Pharmacometrics Syst Pharmacol* 2013; 2: e38.

27. Alfarisi O, Alghamdi WA, Al-Shaer MH, Dooley KE, Peloquin CA. Rifampin vs. rifapentine: what is the preferred rifamycin for tuberculosis? *Expert Rev Clin Pharmacol* 2017; 10: 1027-1036.

28. Dorman SE, Savic RM, Goldberg S, Stout JE, Schluger N, Muzanyi G, Johnson JL, Nahid P, Hecker EJ, Heilig CM, Bozeman L, Feng PJ, Moro RN, MacKenzie W, Dooley KE, Nuermberger EL, Vernon A, Weiner M, Tuberculosis Trials C. Daily rifapentine for treatment of pulmonary tuberculosis. A randomized, dose-ranging trial. *Am J Respir Crit Care Med* 2015; 191: 333-343.

29. Weiner M, Bock N, Peloquin CA, Burman WJ, Khan A, Vernon A, Zhao Z, Weis S, Sterling TR, Hayden K, Goldberg S, Tuberculosis Trials C. Pharmacokinetics of rifapentine at 600, 900, and 1,200 mg during once-weekly tuberculosis therapy. *Am J Respir Crit Care Med* 2004; 169: 1191-1197.

30. Weiner M, Savic RM, Kenzie WR, Wing D, Peloquin CA, Engle M, Bliven E, Prihoda TJ, Gelfond JA, Scott NA, Abdel-Rahman SM, Kearns GL, Burman WJ, Sterling TR, Villarino ME, Tuberculosis Trials Consortium PTBPG. Rifapentine Pharmacokinetics and Tolerability in Children and Adults Treated Once Weekly With Rifapentine and Isoniazid for Latent Tuberculosis Infection. *J Pediatric Infect Dis Soc* 2014; 3: 132-145.

31. Conde MB, Mello FC, Duarte RS, Cavalcante SC, Rolla V, Dalcolmo M, Loredo C, Durovni B, Armstrong DT, Efron A, Barnes GL, Marzinke MA, Savic RM, Dooley KE, Cohn S, Moulton LH, Chaisson RE, Dorman SE. A Phase 2 Randomized Trial of a Rifapentine plus

Moxifloxacin-Based Regimen for Treatment of Pulmonary Tuberculosis. *PLoS One* 2016; 11: e0154778.

32. Keung A, Reith K, Eller MG, McKenzie KA, Cheng L, Weir SJ. Enzyme induction observed in healthy volunteers after repeated administration of rifapentine and its lack of effect on steady-state rifapentine pharmacokinetics: part I. *Int J Tuberc Lung Dis* 1999; 3: 426-436.

33. Pasipanodya JG, McIlleron H, Burger A, Wash PA, Smith P, Gumbo T. Serum drug concentrations predictive of pulmonary tuberculosis outcomes. *J Infect Dis* 2013; 208: 1464-1473.

34. Weiner M, Benator D, Burman W, Peloquin CA, Khan A, Vernon A, Jones B, Silva-Trigo C, Zhao Z, Hodge T, Tuberculosis Trials C. Association between acquired rifamycin resistance and the pharmacokinetics of rifabutin and isoniazid among patients with HIV and tuberculosis. *Clin Infect Dis* 2005; 40: 1481-1491.

35. Gumbo T, Louie A, Deziel MR, Liu W, Parsons LM, Salfinger M, Drusano GL. Concentration-dependent Mycobacterium tuberculosis killing and prevention of resistance by rifampin. *Antimicrob Agents Chemother* 2007; 51: 3781-3788.

36. Gengiah TN, Botha JH, Soowamber D, Naidoo K, Abdool Karim SS. Low rifampicin concentrations in tuberculosis patients with HIV infection. *J Infect Dev Ctries* 2014; 8: 987-993.

37. Gurumurthy P, Ramachandran G, Hemanth Kumar AK, Rajasekaran S, Padmapriyadarsini C, Swaminathan S, Venkatesan P, Sekar L, Kumar S, Krishnarajasekhar OR, Paramesh P. Malabsorption of rifampin and isoniazid in HIV-infected patients with and without tuberculosis. *Clin Infect Dis* 2004; 38: 280-283.

38. Jeremiah K, Denti P, Chigutsa E, Faurholt-Jepsen D, PrayGod G, Range N, Castel S, Wiesner L, Hagen CM, Christiansen M, Changalucha J, McIlleron H, Friis H, Andersen AB. Nutritional supplementation increases rifampin exposure among tuberculosis patients coinfected with HIV. *Antimicrob Agents Chemother* 2014; 58: 3468-3474.

Figure Legends

Figure 1. PRISMA Flow Diagram.

Figure 2. Final rifapentine pharmacokinetic-enzyme model. The number of transit compartments (NN) was estimated using the relationship of $k_{TR} = (NN+1)/MTT$, where MTT is the mean transit time and k_{TR} is the transit rate constant. The absorption rate constant (k_a) was assumed equal to k_{TR}. Rifapentine autoinduction was modeled with an enzyme turnover model, where the effect (EFF) of rifapentine concentration in the central compartment increased the enzyme production rate (k_{ENZ}), thereby increasing the enzyme pool (ENZ). Rifapentine clearance (CL) increased as a result of increased ENZ. V is the apparent volume of distribution. The fraction of the drug absorbed (F; relative bioavailability) increased (+) or decreased (-) as indicated.

Figure 3. Rifapentine autoinduction profile. (A) The sigmoid relationship between rifapentine concentration and autoinduction is shown in the black line. Dashed lines represent the average concentration at steady state of daily therapy with 300 mg (yellow), 450 mg (green), and 600 mg (navy) of rifapentine in a typical HIV-negative individual. (B) Rifapentine induction over time following daily administration of 600 mg. Black dashed line represents the time at which the induction process reaches steady state.

Figure 4. Validation of the structural rifapentine population pharmacokinetic model. Prediction-corrected visual predictive check (VPC) of base model with (A) analysis dataset, (B) validation dataset, and (C) combined dataset. Figures show the model predictions (shaded areas)

compared to observed/raw rifapentine concentrations (dots). Model predictions were based on the base structural model, built from the analysis dataset alone. The 5th (dashed line), 50th (solid line), 95th (dashed line) percentiles of the observed raw data are overlaid onto the 95% confidence intervals of model-predicted concentrations at the 50th (light blue), and 5th and 95th (dark blue) percentiles, obtained from 500 simulations of each respective dataset.

Figure 5. Relationship between weight and rifapentine clearance. The relationship was assessed for (A) all subjects and (B) only DS-TB and LTBI patients with final model parameter estimates. Dashed line represents loess regression curve.

Figure 6. Effect of dose and dosing frequency on rifapentine exposure. (A) Rifapentine concentration over time, and (B) concentration over time in log-scale, in a typical HIV-uninfected individual following once daily, thrice weekly, twice weekly, and once weekly administration of 600 mg (yellow), 900 mg (green), or 1200 mg (dark blue). Black dashed line = minimum inhibitory concentration (MIC; equal to 0.06 mg/L)

Figure 7. Pharmacokinetic profiles of rifapentine following (A) 1HP and (B) 3HP regimens. Concentration-time profiles over 24 hours are shown for the typical adult by HIV status on (A) day 21 of therapy, to reflect steady state concentrations, and (B) after first dose since no accumulation occurs with weekly dosing.

Figure 8. Predicted rifapentine exposures with different dosing methods for (A) 1HP and (B) 3HP regimens. Drug exposure over 24 hours (AUC_{0-24h}) profiles are based on 500

simulations. (A) 1HP predictions reflect steady state exposures to account for autoinduction. 'Weight band' rifapentine doses were 300 mg for < 35 kg, 450 mg for 35-45 kg, and 600 mg for >45 kg, as currently recommended for 1HP. The 'Flat' approach prescribed 600 mg to all individuals, and 'HIV stratified' increased dose in HIV-positive to 750 mg. (B) 3HP doses were 750 mg for <50 kg and 900 mg for 50+ kg for the 'weight band' approach, as currently recommended. The 'Flat' approach prescribed 900 mg to all individuals, and 'HIV stratified' increased dose in HIV-positive to 1200 mg. Gray dashed lines represent (B) the median AUC_{0-24h} (=317 mg*h/L) observed in patients treated with 3HP in the PREVENT-TB trial (i.e., TBTC-26) and (A) the median predicted AUC_{0-24h} in HIV-positive patients with 600 mg daily (=219 mg*h/L).

Figure 9. Predictors of month 2 culture conversion. Data were acquired from two Phase II clinical studies (TBTC29, TBTC29x) where participants received 10 mg/kg rifapentine daily. Odds ratios are from univariate analysis.

Tables

Table 1. Baseline characteristics of the study participants in the pooled datasets.

Trial[*] (Ref)	Rifapentine Regimen	N Individuals, (N samples)	Age, yr	Weight, kg	Female sex	HIV-positive
Analysis cohort						
06-0050 (19) Phase 1 HV PM	900 mg thrice weekly with low fat meal	14, (269)	41 (24-64)	76 (50-97)	3 (21.4)	-
Rifaquin (12) Phase 3 DS-TB PM	900 mg twice weekly or 1200 mg once weekly with high-fat meal	241, (846)	32 (18-80)	56 (38-78)	88 (36.5)	46 (19.1)
TBTC-29B (14) Phase 1 HV P[Mdz]	5 - 20 mg/kg once daily with low-fat meal	26, (504)	47 (24-60)	82 (60-99)	5 (19.2)	-
TBTC-25 (29) Phase 2 DS-TB PH	600, 900, or 1200 mg once weekly on empty stomach	35, (357)	44 (18-68)	65 (46-110)	12 (34.3)	-
ACTG-A5311 (21) Phase 1 HV P	10 mg/kg twice daily or 15 or 20 mg/kg once daily with low- or high-fat meal	44, (1210)	35 (20-59)	82 (60-99)	12 (27.3)	-
Validation cohort						
TBTC-29X (28) Phase 2 DS-TB PHZE	10, 15, or 20 mg/kg once daily with high-fat meal	225, (713)	30 (18-70)	55 (40-83)	66 (29.3)	19 (8.4)
TBTC-26 (30) Phase 3 LTBI	900 mg once weekly with food	77, (77)	40 (19-63)	81 (49-169)	37 (48.1)	-

28

PH

TBTC-29 (22) Phase 2 DS-TB PHZE	10 mg/kg 5 days per week on empty stomach	158, (158)	36 (18-86)	60 (40-101)	46 (29.1)	16 (10.1)
RioMar (31) Phase 2 DS-TB PHMZ	7.5 mg/kg once daily with food	43, (167)	-	58 (45-83)	NR	-

Data are expressed as median (range) or number (percentage).

[*] A description of each trial is below including study phase, population, and drug regimen.

Definition of abbreviations: NR = not recorded; HV= healthy volunteers; DS-TB = drug-sensitive tuberculosis; LTBI = latent tuberculosis infection; P = rifapentine; H = isoniazid. M = moxifloxacin; [Mdz] = midazolam, only administered in some of the study participants; Z = pyrazinamide; E = ethambutol.

Table 2. Final parameter estimates for the rifapentine population pharmacokinetic model.

Parameter	Population Estimate		Inter-individual variability	
	Value [%RSE]	95% CI[†]	%CV [%RSE]	95% CI[†]
CL/F (L/h)	1.11 [1.92]	0.952 - 1.48	24.3 [9.34]	12.8 - 28.0
V/F (L)	36.7 [1.99]	28.5 - 40.9	17.6 [17.7]	10.5 - 24.0
MTT (h)	1.94 [2.97]	1.83 - 2.04	-	-
NN	2.15 [5.44]	1.66 - 2.70	-	-
Bioavailability	100 *fixed*	-	29.8 [10.8]	21.5 - 34.6
Fixed effects on bioavailability[‡]				
Dose	0.0167 [5.30]	0.00343 - 0.0287	-	-
HIV infection	0.729 [6.26]	0.584 - 0.815	-	-
High-fat meal	1.49 [3.05]	1.37 - 1.64	-	-
Fasting	0.731 [5.51]	0.546 - 0.776	-	-
k_{ENZ} $(h^{-1})^{*, \parallel}$	0.00587 [32.1]	0.00291 - 0.0135	-	-
E_{max} (%)[*]	73.0 [25.2]	51.0 - 116	-	-
EC_{50} (mg/L)[*]	4.27 [39.8]	1.80 - 6.57	-	-
γ	10 *fixed*	-	-	-
Residual error of rifapentine	0.577 [4.13]	0.573 - 0.699	-	-
CL_m/f_m (L/h)	3.11 [12.2]	1.89-6.26	40.0 [6.69]	34.2-44.6
V_m/f_m (L)	2.15 [7.07]	1.67-3.15	-	-
$f_{m, dose}$[**]	0.0185 [3.56]	0.0004 -0.0266	-	-
HIV effect on CL_m	1.36 [9.85]	-	-	-
Residual error of metabolite	0.631 [5.59]	0.560-0.695	-	-

[*] autoinduction parameters were estimated based on the analysis dataset alone.

[†] Confidence intervals were based on 926 (out of 1000) successful bootstrap runs for rifapentine model and 999 (out of 1000) successful bootstrap runs for metabolite model.

[‡] Fixed effects on bioavailability (F) were relative to HIV-negative individuals taking 300 mg of rifapentine with a low-fat meal, where F=1 for each reference condition. Relative bioavailability is calculated as: $F=F_{dose}*F_{HIV}*F_{high-fat}*F_{fasting}$, where F_{dose} is the relative reduction in bioavailability per 100 mg above 300 mg (equal to 1- estimate*(dose/100 mg), F_{HIV} is the relative bioavailability in HIV-positive

individuals, $F_{high-fat}$ is the relative bioavailability with a high-fat meal (vs. low-fat meal), and $F_{fasting}$ is the relative bioavailability with fasting (vs. low-fat meal).

$\parallel$ Translates to an enzyme turnover half-life of 118 hours.

** Fraction metabolized is a function of dose, where $f_m = 1 - f_{m,dose}*(dose/100 \text{ mg})$.

Definition of abbreviations: RSE=relative standard error; CI=confidence interval; CV=coefficient of variation; CL/F=apparent clearance; V/F=apparent volume of distribution; MTT=mean transit time; NN=number of transit compartments; k_{ENZ}=enzyme production rate; EC_{50}=concentration where effect is 50% of maximum; E_{max}=maximum effect; γ =steepness for E_{max} equation; CL_m/f_m =metabolite clearance; V_m/f_m =metabolite volume of distribution; $F_{m,dose}$= dose-dependent reduction in fraction metabolized.
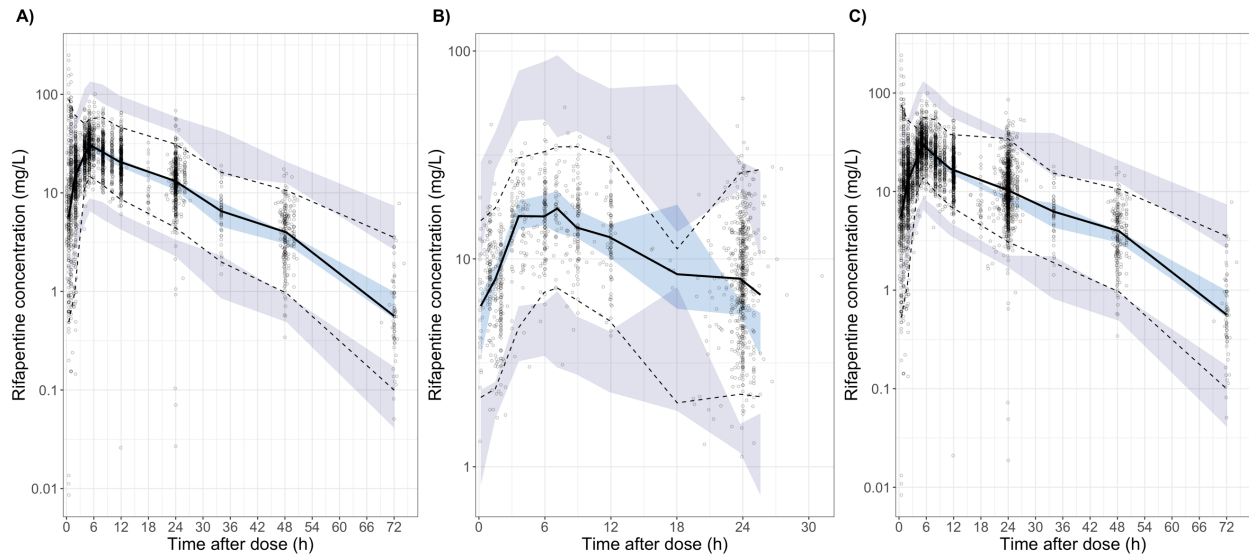
Figures

Figure 1. PRISMA Flow Diagram
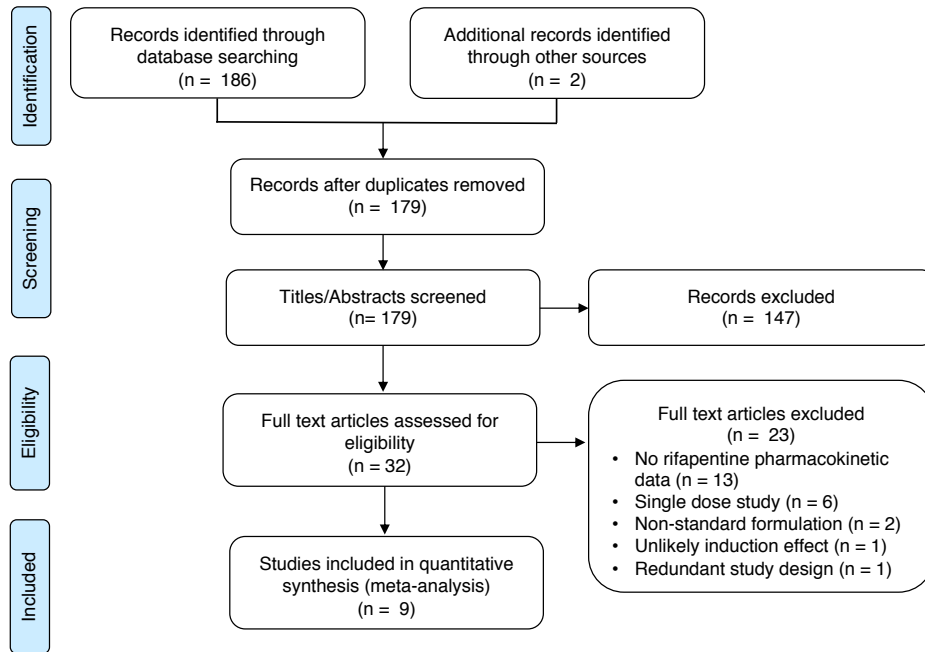
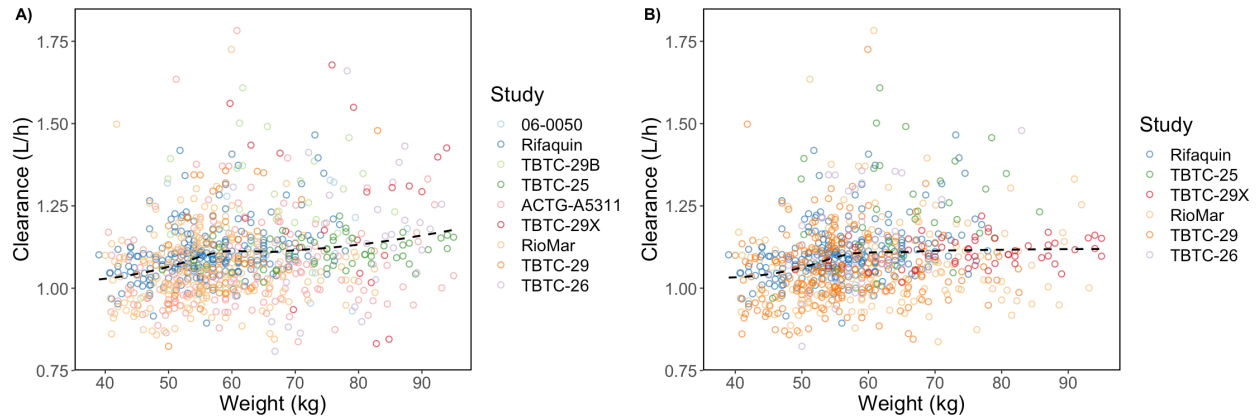## Figure 2. Final rifapentine pharmacokinetic-enzyme model.
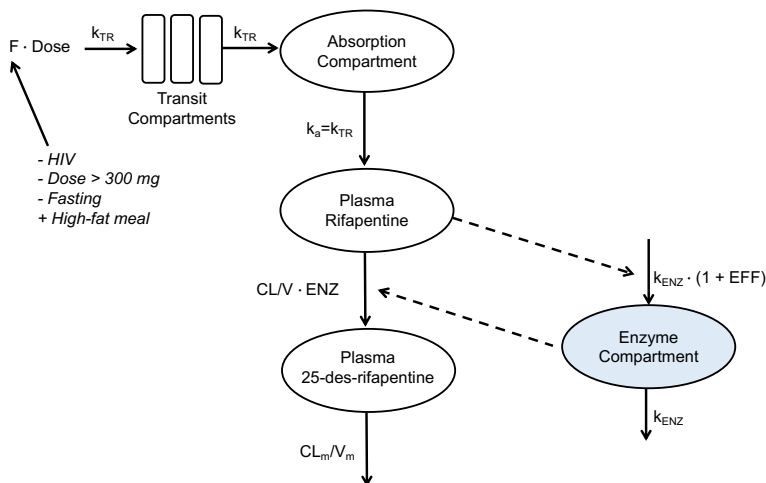
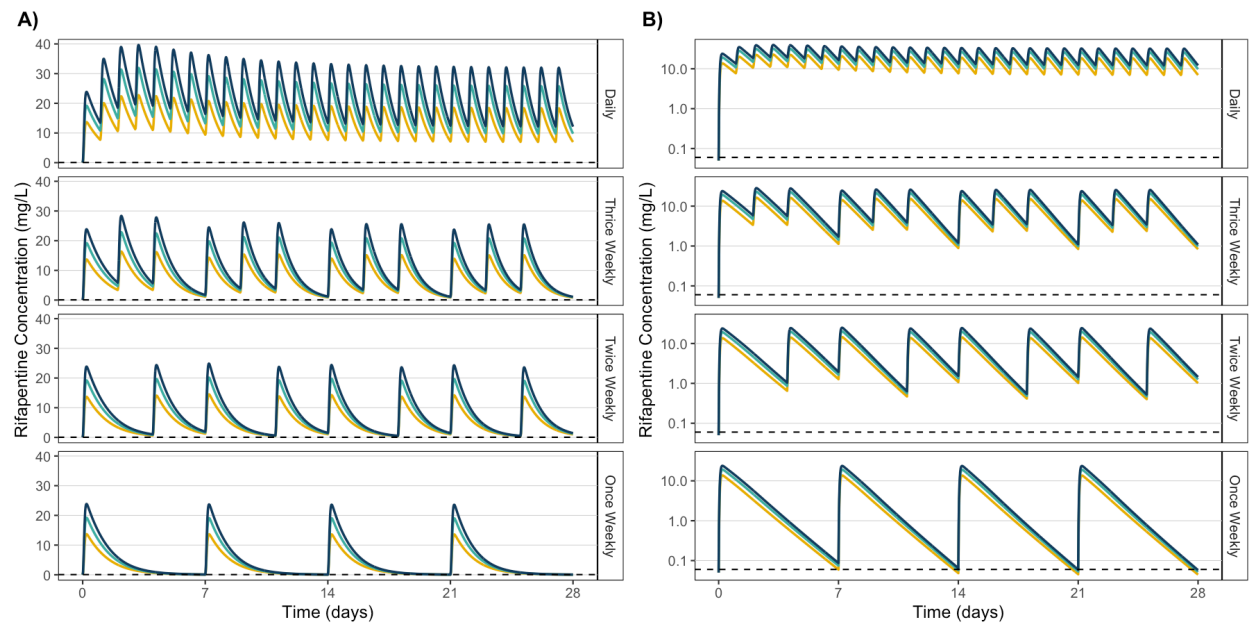**Figure 3. Rifapentine autoinduction profile.**
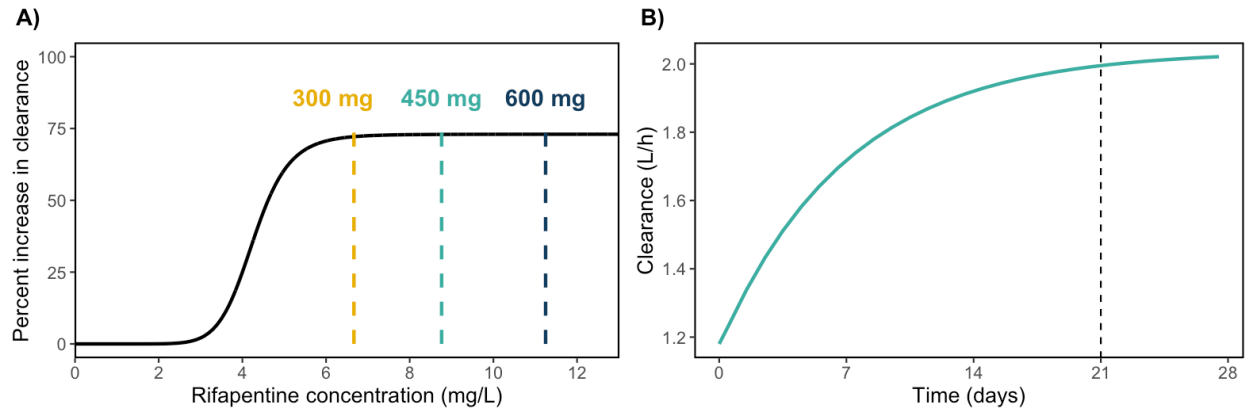
Figure 4. Validation of the structural rifapentine population pharmacokinetic model.
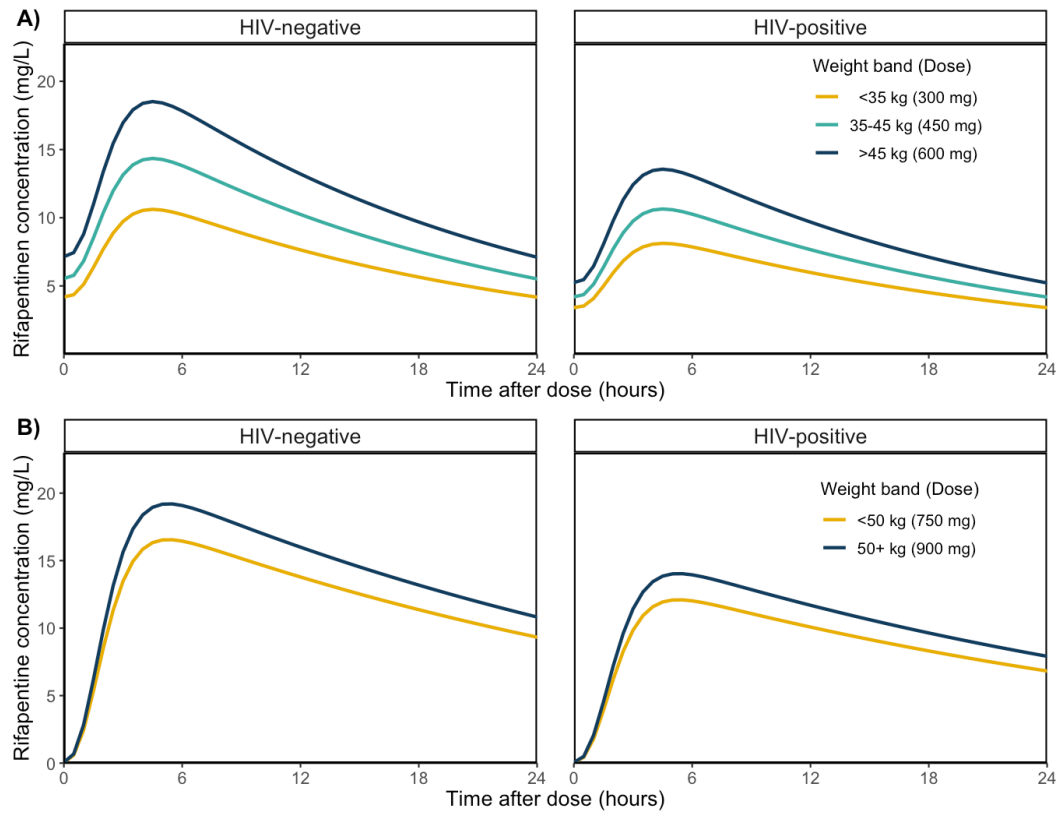
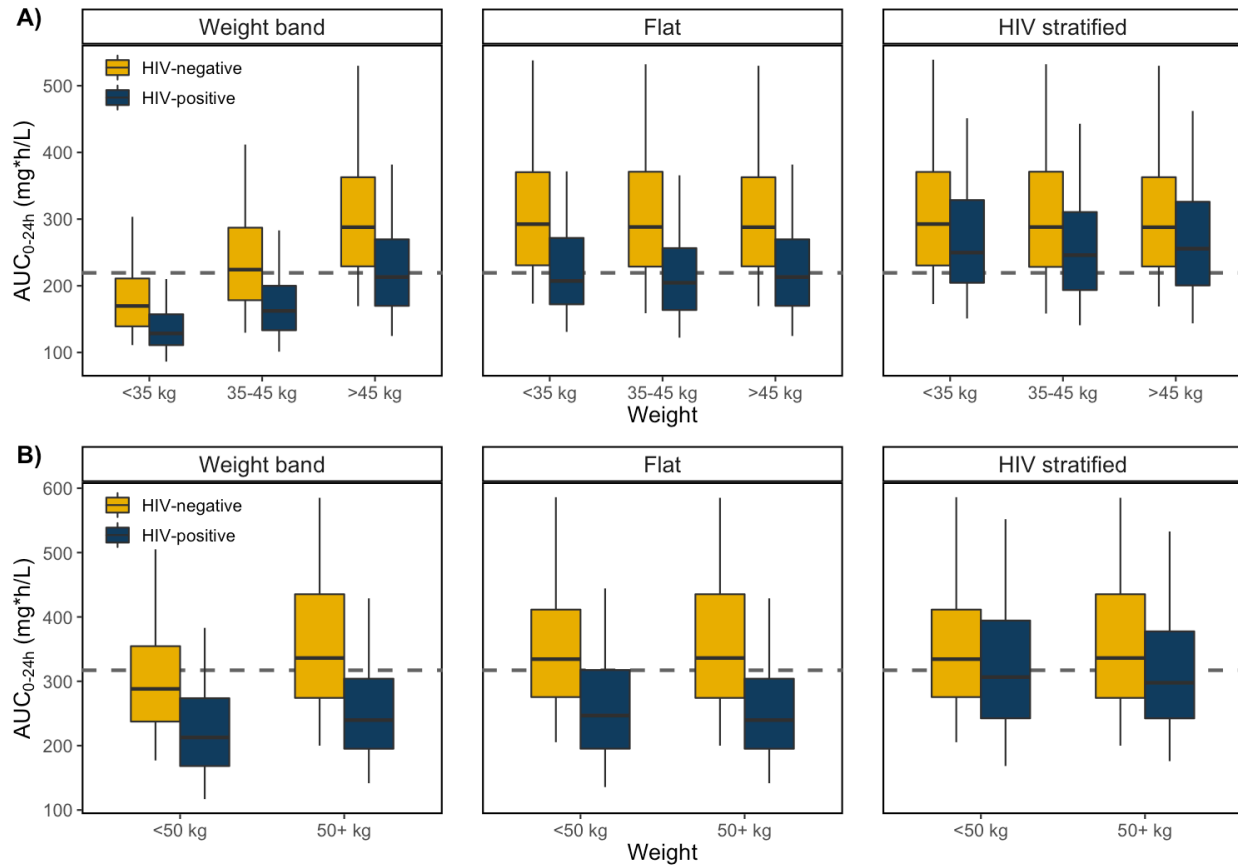**Figure 5. Relationship between weight and rifapentine clearance.**

Figure 6. Effect of dose and dosing frequency on rifapentine exposure.

Figure 7. Pharmacokinetic profiles of rifapentine following (A) 1HP and (B) 3HP regimens.

Figure 8. Predicted rifapentine exposures with different dosing methods for (A) 1HP and (B) 3HP regimens.

Figure 9. Predictors of month 2 culture conversion.